

Computation of FM Distortion in Linear Networks for Bandlimited Periodic Signals

By CLYDE L. RUTHROFF

(Manuscript received December 14, 1967)

Computations of the distortion generated in passing large-index, frequency-modulated signals through symmetrical single-pole and three-pole bandpass filters are presented. The computation is for a bandlimited periodic modulation signal; noise modulation is simulated by the use of periodic noise samples in a Monte Carlo procedure.

The convergence of the Monte Carlo procedure is illustrated for the case of the single-pole filter and the results are in good agreement with measurements.

Computations of envelope distortion are also presented. These data give the amplitude-to-phase conversion in the receiver containing the filter to within a constant factor, the constant being the AM/PM conversion coefficient of the limiter.

I. INTRODUCTION

In spite of the efforts of a large number of investigators who have studied the problem over three decades there is no way to compute the distortion caused by filters and other networks for arbitrary angle modulated signals of large index or large baseband bandwidths. However, by use of the Fourier method¹⁻⁴ introduced by Roder in 1937, it is possible to compute the exact responses of networks to a frequency-modulated signal for bandlimited periodic modulation signals.

In addition to deterministic signals of this class, noise modulation can also be simulated and the resulting network distortion computed by a Monte Carlo procedure. In an excellent paper, Medhurst and Roberts⁴ have described the procedure and given some results for low index FM, pre-emphasized in accordance with CCIR standards.

Their computer program was written in Extended Mercury Autocode. The same method, coded in FORTRAN II, and extended to include the effects of amplitude as well as phase distortion is being used to study large index FM systems.

The results presented are for single sine wave modulation and random noise modulation.

II. ANALYSIS

The modulating signals are restricted to those which are both bandlimited and periodic. This class includes many signals used for test purposes; the notable exception is the signal consisting of band-limited Gaussian noise. More will be said of noise modulation later.

The analysis and computational procedure follows that of Medhurst and Roberts in Ref. 4 and is outlined briefly here. Specifically, the signals are those which can be written as finite Fourier series.

$$\mu(t) = \sum_{n=1}^N (a_n \cos n\omega_a t + b_n \sin n\omega_a t) \text{ radians}, \quad (1)$$

where:

$$\omega_a = 2\pi f_a = 2\pi/T,$$

T is the period of $\mu(t)$,

$$a_n = \frac{2}{T} \int_{-T/2}^{T/2} \mu(t) \cos n\omega_a t \, dt,$$

$$b_n = \frac{2}{T} \int_{-T/2}^{T/2} \mu(t) \sin n\omega_a t \, dt.$$

If $\mu(t)$ is the desired phase modulation, or $\mu'(t) = d\mu(t)/dt$ the frequency modulation, the angle-modulated signal is

$$e = (2)^{\frac{1}{2}} \cos [\omega_c t + \mu(t)] \quad (2)$$

where ω_c is the carrier frequency in radians per second. The FM signal of (2) has a line spectrum with lines at $\omega_c \pm M\omega_a$, $M = 1, 2, 3, \dots$. The lines always occur at these frequencies, changing only in amplitude and phase as functions of a_n , b_n . It is this feature which makes possible a digital computer solution and, conversely, is the reason for restricting the form of the modulating signal to that of $\mu(t)$ in (1). Beginning with (1) and (2) the major steps in the analysis are:

- (i) Derive the line spectrum of (2).

- (ii) Modify the lines in amplitude and phase in accordance with the response of the network being studied.
- (iii) Derive the envelope and phase of the modified line spectrum, that is, determine $E(t)$ and $\theta(t)$ where the output of the network is written

$$e_o = E(t) \cos [\omega_c t + \theta(t)] \quad (3)$$

- (iv) Derive the line spectrum of $E(t)$, $\theta(t)$, and $d\theta/dt$.

III. RANDOM MODULATION

An important measuring method in widespread use on FM systems is the noise loading test. The importance of this method arises from the fact that a band of thermal noise is a good approximation to a frequency division multiplex signal which consists of a number of voice channels. In this test a band of thermal noise in the frequency range $0-W$ Hz is the baseband signal. The noise is removed by band rejection filters in one or more narrow bands or slots ahead of the modulator. At the receiver the power density appearing in the slots is a measure of the intermodulation distortion in the system. The results are usually given in the form of a signal-to-distortion ratio, the signal being the power density at the slot frequency when the band rejection filter is removed, that is, when the signal is present.

Computations of distortion can be made along these lines by following a Monte Carlo procedure with a sequence of random noise samples generated from the periodic form of (1). A set of N sine waves of equal amplitudes and random phases distributed uniformly in the interval $0 - 2\pi$ constitutes the basic signal. Figure 1 is an example of this random noise sample for $N = 10$ and Fig. 2 for $N = 50$. One or more amplitudes are set to zero to form the slots, and the power in the slots as a result of network distortion is computed as outlined in Section II. The process is repeated with a sequence of random noise samples, each sample with a set of N independent random phases. The distortion is averaged for the final result. If N is large enough, if the number of sets is large enough, and if the network transfer function is well-behaved, then the results approach those obtained in a noise loading test.

Rice⁵ has shown that such a noise representation has a normal amplitude distribution as $N \rightarrow \infty$ and $\omega_a \rightarrow 0$. Bennett⁶ has computed the amplitude distribution as a function of N . The conclusion is that with respect to amplitude distribution the sets of random signals of the

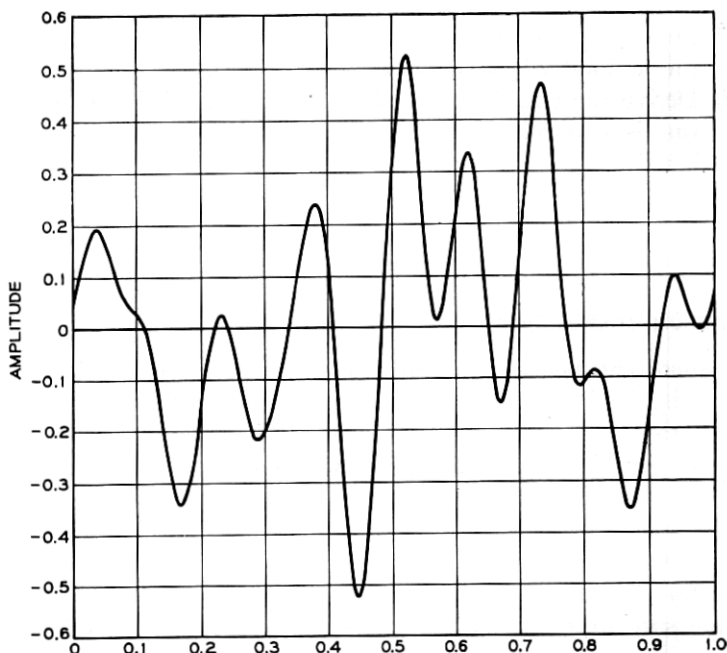


Fig. 1—A periodic random noise sample for $N = 10$. Peak amplitude/rms amplitude = $|-0.525|/[1/(2N)^{1/2}] = 2.34$.

form (1) approximate Gaussian noise. With respect to the spectrum the situation is otherwise; the spectrum of noise is continuous whereas the simulation, for finite N , has a line spectrum. This means that the results computed with the simulated noise will approximate the results for real noise only for network responses which are smooth enough. An example of a function which is not smooth enough is a network response of unity at the spectral lines and zero elsewhere. In spite of this limitation it is not expected that smoothness will be a serious problem for most cases of interest.

3.1 Modulation Index

The modulating signal $\mu(t)$ can be written as follows:

$$\mu(t) = \sum_{n=1}^N A_n \cos(n\omega_a t + \alpha_n) \text{ radians}, \quad (4)$$

where,

$$A_n^2 = a_n^2 + b_n^2$$

$$\alpha_n = -\tan^{-1} \frac{b_n}{a_n}.$$

The baseband is

$$W = N\omega_a. \quad (5)$$

Using (4) to simulate noise in a phase modulation system, the amplitudes A_n are equal and the random phases α_n are uniformly distributed from 0 to 2π . If the rms phase deviation is φ radians,

$$A_n = \varphi(2/N)^{\frac{1}{2}} \text{ radians.} \quad (6)$$

For the FM application the amplitude terms of the frequency modulation $\mu'(t)$ are made equal to simulate a flat band of noise, that is, $n\omega_a A_n = \Delta$, the peak frequency deviation per sine wave. The mean

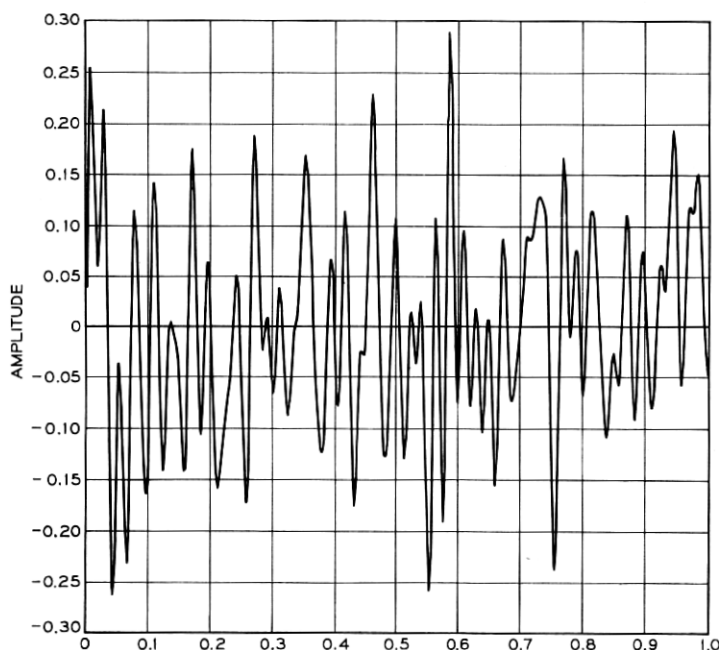


Fig. 2 — A periodic random noise sample for $N = 50$. Peak amplitude/rms amplitude = $|0.29|/[1/(2N)^{1/2}] = 2.90$.

square frequency deviation is

$$\sigma^2 = \frac{\Delta^2}{2} N = \frac{n^2 \omega_a^2 A_n^2}{2} \times N.$$

Substituting for ω_a from (5) we get

$$A_n = (\sigma/W)[(2N)^{1/2}/n]. \quad (7)$$

The rms phase and frequency deviations can be related to the RF bandwidth by Carson's rule which, for noise modulation, is written

$$B = 2W(1 + 4\sigma/W), \quad (8)$$

where the peak frequency deviation is assumed to be 4σ . Suppose that the line spectrum of (2) contains kN lines in addition to the carrier, then the bandwidth of the computed spectrum is

$$B = kN\omega_a. \quad (9)$$

From (5), (8), and (9) we get the relation between k and σ

$$k = 2(1 + 4\sigma/W). \quad (10)$$

This equation is as accurate as Carson's rule and is useful for estimating k when σ/W is given. If k is chosen too small, significant spectral components are omitted from the spectrum; the effect is to pass the complete spectrum through an ideal filter of bandwidth $kN\omega_a$.

In a similar manner k and φ can be related for the phase modulation case. The rms frequency deviation for the PM case is given by

$$\frac{\sigma}{W} = \varphi \sqrt{\frac{1 + \frac{3}{2N} + \frac{1}{2N^2}}{3}} \quad (11)$$

where N is the number of tones in the baseband. Substitution of (11) into (10) gives the desired result.

3.2 Limitations on Modulation Index

It has been shown (9), that the maximum RF spectrum bandwidth is given by $B = kN\omega_a$. From (5) the baseband bandwidth is $W = N\omega_a$. Assuming that only negligible energy falls outside B , then B is the RF bandwidth and the parameter k is a bandwidth expansion factor since

$$k = B/W. \quad (12)$$

Now, k and the rms frequency deviation σ are related by (10). The product kN is limited by the high speed storage capacity of the machine;

this implies a relationship between N and σ/W . Let $M \geq kN$ be the maximum value of kN which can be accommodated in the machine. Then,

$$\sigma/W \leq 1/4(M/2N - 1). \quad (13)$$

This expression is dependent upon Carson's rule and has the same unknown precision—but it serves to demonstrate the point that if large σ/W is desired, N must be made small. In the work reported here, $M = 500$ so that for $N = 10$, $\sigma/W \leq 6$. Conversely for $N = 100$, $\sigma/W \leq 0.375$.

Because Carson's rule has an unknown precision it is necessary to determine to reasonable accuracy the relationship between k and σ/W . With a perfect rectangular filter of bandwidth $kN\omega_a$, signal-to-distortion ratios have been computed for the case $N = 10$. In these computations, slots 1 and 10 were set to zero separately and the SDR computed for that slot.

The results are shown in Fig. 3 as a function of σ/W with the bandwidth expansion ratio k as a parameter. In all cases slot 1 has the lowest

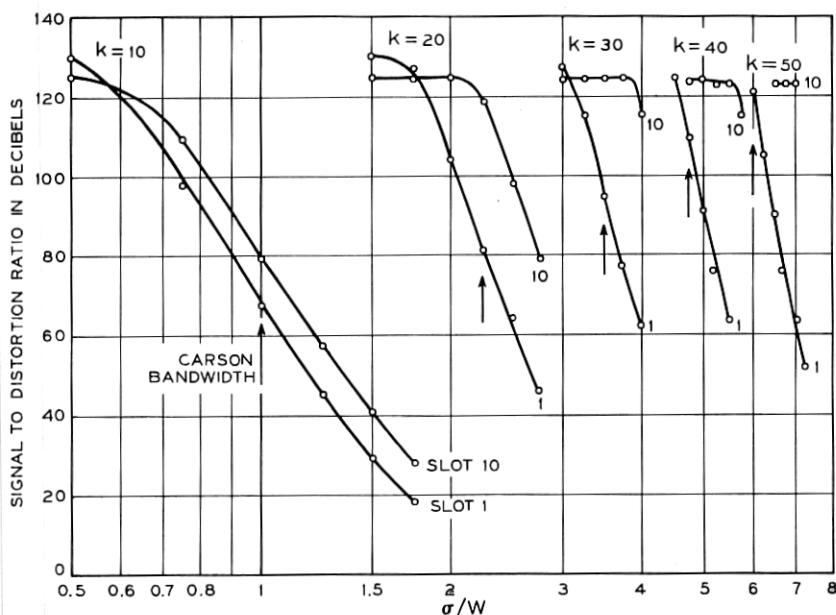


Fig. 3 — FM signal-to-distortion ratios for square filters containing $kN+1$ spectral lines and with $N = 10$.

SDR. The levelling off for SDR near 124 dB is probably caused by the computer round-off error. The negative slopes are the result of the finite filter bandwidth of $kN\omega_a$ and the decreasing accuracy of the method of harmonic interpolation in approximating the spectrum. Increasing k improves the accuracy of the approximation.

Values of σ/W obtained from Carson's rule in the form given in (10) are shown by the arrows in Fig. 3. Fig. 3 can be used to determine the value of k required to compute the SDR for a given σ/W . In all examples reported here, k and N have been chosen so that without a filter an $\text{SDR} \geq 100$ dB was obtained for the values of σ/W used. The data of Fig. 3 are averages of 20 noise samples.

IV. THE SINGLE POLE FILTER

The single-pole filter is the simplest possible realizable bandpass filter and is important for two reasons.

(i) It is widely used. For example, it is nearly optimum for use in the IF section of a frequency feedback receiver.⁷

(ii) As simple as it is, no previous method is adequate for the computation of FM distortion for high frequencies and large deviations.

4.1 *Single Sine Wave Modulation*

A number of years ago Bodtmann⁸ made extensive measurements on a single-pole filter with both single sine wave and noise modulation.* Let us compare the measured and computed results.

The transfer function of a narrow band single-pole filter is

$$Y = \frac{1}{1 + j \frac{f - f_0}{f_c}} \quad (14)$$

where:

f_0 is the center frequency and

f_c is the half bandwidth, that is, the frequencies at which the response is down 3 dB are $f_0 \pm f_c$.

Bodtmann's filter was centered near 70 MHz with a half bandwidth of 1.223 MHz. The skirts fit the response of (14) to within ± 0.1 dB out to the 15 dB loss points. The measured and computed ratios of signal-to-third harmonic distortion power are shown in Fig. 4. Notice

* It was Bodtmann's results which led to the discovery of a simple error in existing theories.⁹⁻¹¹

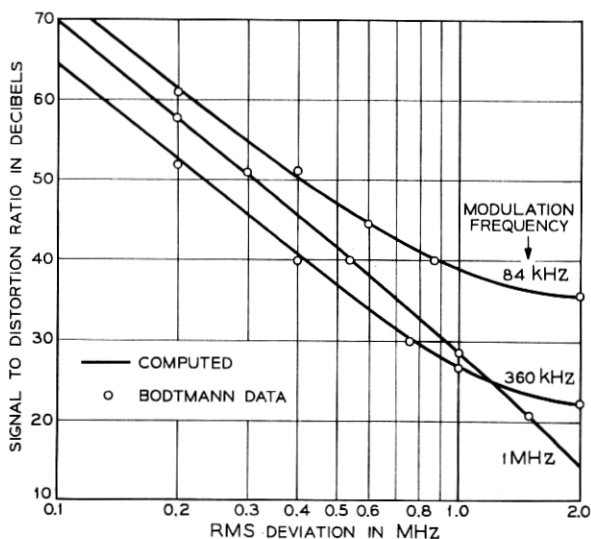


Fig. 4 — Third harmonic distortion in single pole filter.

the peculiarity which occurs at a deviation of 1.2 MHz where the curves for 360 KHz and 1 MHz modulation frequencies cross. Existing theories do not predict this behavior which is verified here by direct computation.

4.2 Results for Random Modulation

Computations of SDR have been made for a single pole filter for the random modulation discussed in Section III. The results, for noise samples of 10 and 50 sine waves of equal amplitude and random phase, are shown in Fig. 5 with Bodtmann's measured results. The computations followed the Monte Carlo procedure described previously. The data in Fig. 5 for $N = 50$ is the average over two slots at each frequency for 50 noise samples. The pairs of slots are 4 and 5, 17 and 19, and 49 and 50, corresponding to the slot frequencies 84 KHz, 360 KHz and 1 MHz, respectively. Data for all the slots were computed in the same computer run. In the computations for $N = 10$ one slot at a time was computed, each point being the average of 80 noise samples.

When the noise sample is simulated by 50 sine waves, the agreement with the experimental data is good. The SDR's for the case of 10 sine waves per noise sample are somewhat higher reflecting the

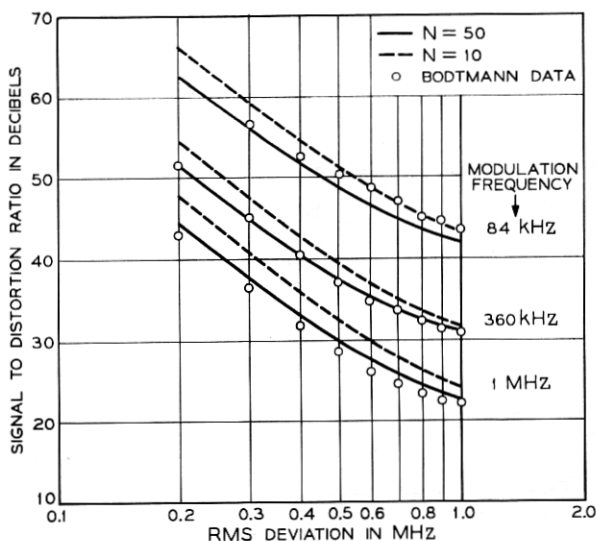


Fig. 5 — Bodtmann's measured results compared with noise samples.

fact that larger modulation peaks are to be found in the sample with the larger number of sine waves.⁶

4.3 Convergence of the Monte Carlo Process

The SDR's of 80 individual noise samples for $N = 10$ are shown in Fig. 6 in four sets of 20 each. The average SDR as a function of

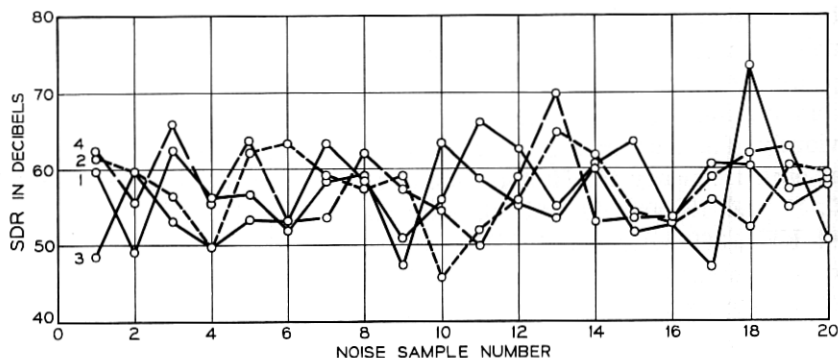


Fig. 6 — FM SDR in a single pole filter. Ten sine waves in baseband; SDR computed in slot 4; bandwidth expansion factor $k = 10$; $\sigma = 0.2$ MHz; $\omega_c/W = 1.223$.

the number of noise samples is shown in Fig. 7; the four sets of Fig. 6 are averaged in sequence. It is interesting to ask how close to the 80-sample average one would get if only 20 samples were used. As a partial answer, the four sets of Fig. 6 were averaged separately and the results are shown in Fig. 8. All four 20-sample averages fall within 1 dB of the 80-sample average.

Similar data for slot 19 is presented for the case $N = 50$ in Figs. 9, 10, and 11. Slot 17 was also computed and the averages for both slots are shown in Figs. 12 and 13. The results for slots 17 + 19 are remarkably similar to those of 19 alone. The 10-sample averages deviate from the 50 sample average by a maximum of 2.7 dB for slot 19 and 2.3 dB for the sum of slots 17 + 19. Interestingly enough, the 10-sample average for $N = 10$ deviates from the 80-sample average by a maximum of 2.2 dB.

The behavior of the SDR of a single noise sample as a function of σ/W is also of interest. Fig. 14 shows this behavior for each of the first six noise samples of set 1, Fig. 6, compared with the 80-sample

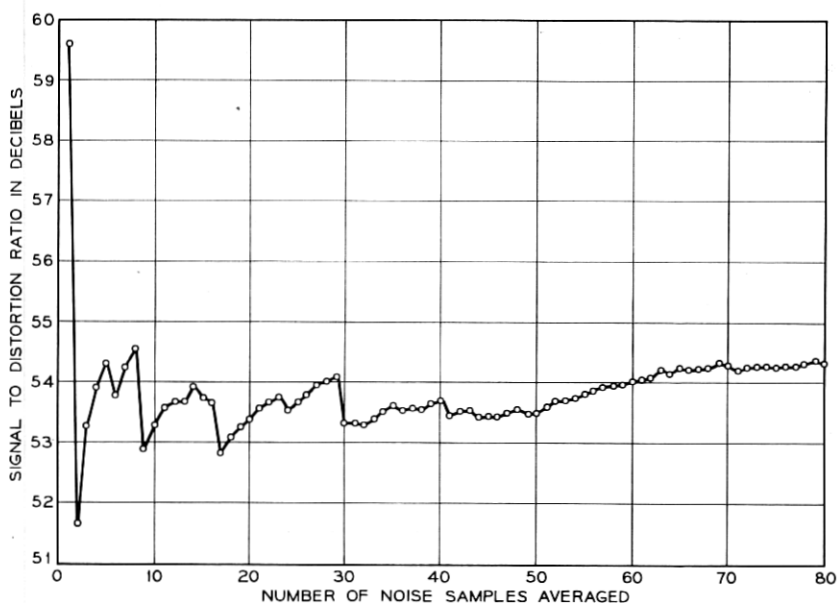


Fig. 7 — Fluctuations in SDR of single pole filter as a function of number of sets of computations. Ten sine waves in baseband; SDR computed in slot 4; bandwidth expansion factor $k = 10$; $\sigma = 0.2$ MHz; $\omega_c/W = 1.223$.

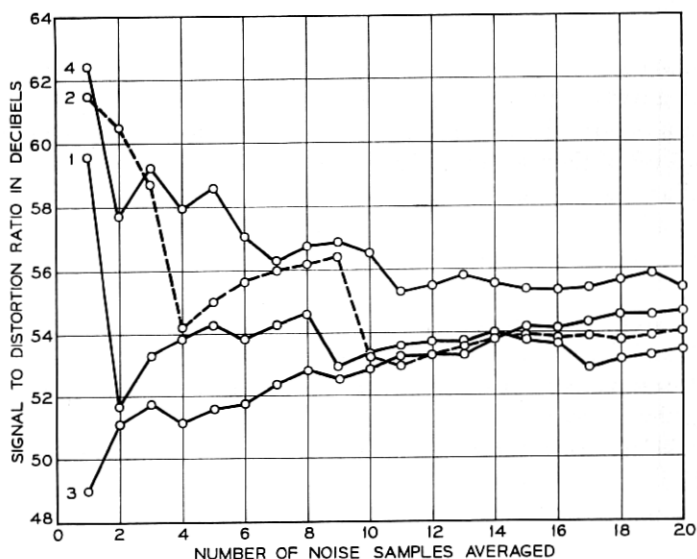


Fig. 8—Fluctuations in SDR of single pole filter as a function of number of sets of computations. Ten sine waves in baseband; SDR computer in slot 4; bandwidth expansion factor $k = 10$; $\sigma = 0.2$ MHz; $\omega_c/W = 1.223$.

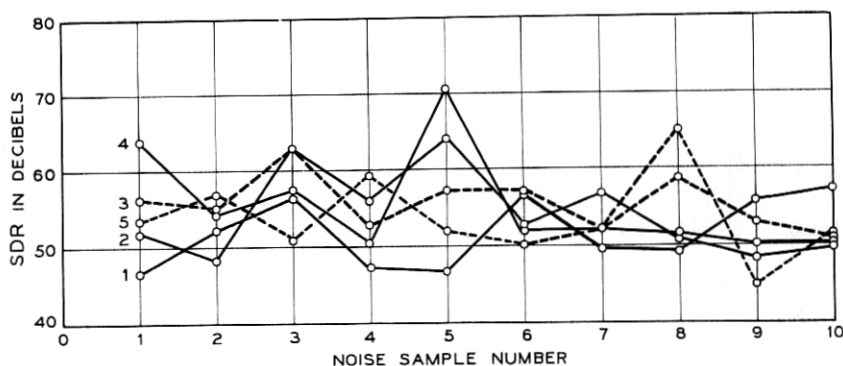


Fig. 9—FM SDR in a single pole filter. 50 sine waves in baseband; SDR computed in slot 19; bandwidth expansion factor $k = 10$; $\sigma = 0.2$ MHz; $\omega_c/W = 1.223$.

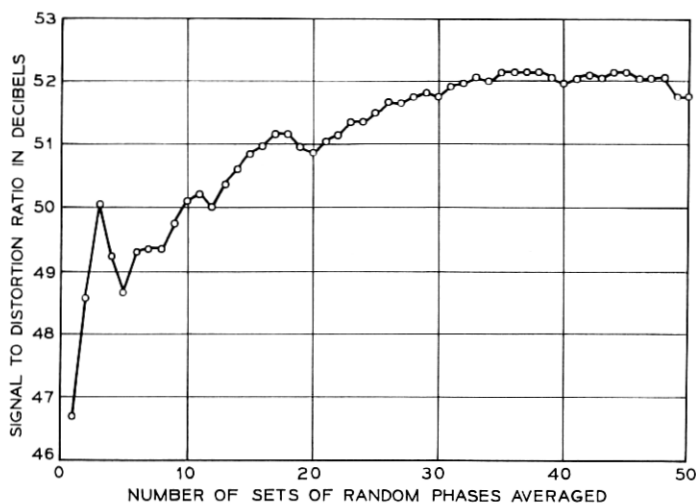


Fig. 10—Fluctuations in SDR of single pole filter as a function of number of sets of computations. 50 sine waves in baseband; SDR computed in slot 19; bandwidth expansion factor $k = 10$; $\sigma = 0.2$ MHz; $\omega_c/W = 1.223$.

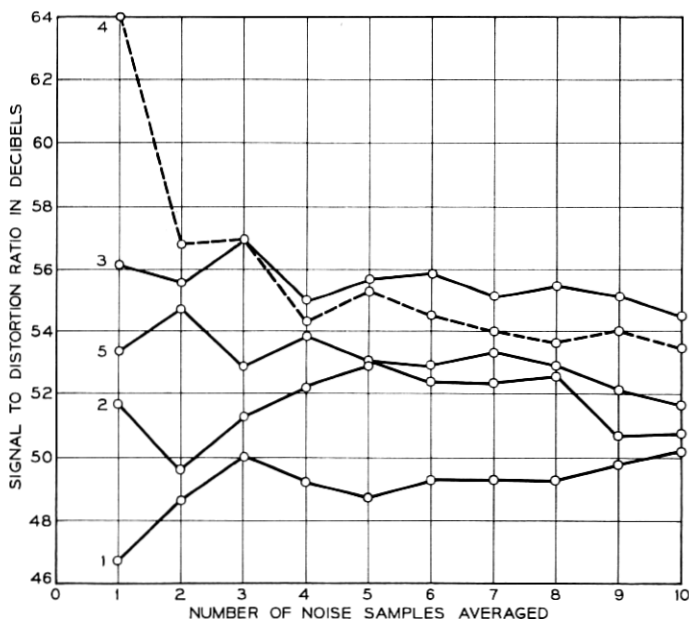


Fig. 11—Fluctuations in SDR of single pole filter as a function of number of sets of computations. 50 sine waves in baseband; SDR computed in slot 19; bandwidth expansion factor $k = 10$; $\sigma = 0.2$ MHz; $\omega_c/W = 1.223$.

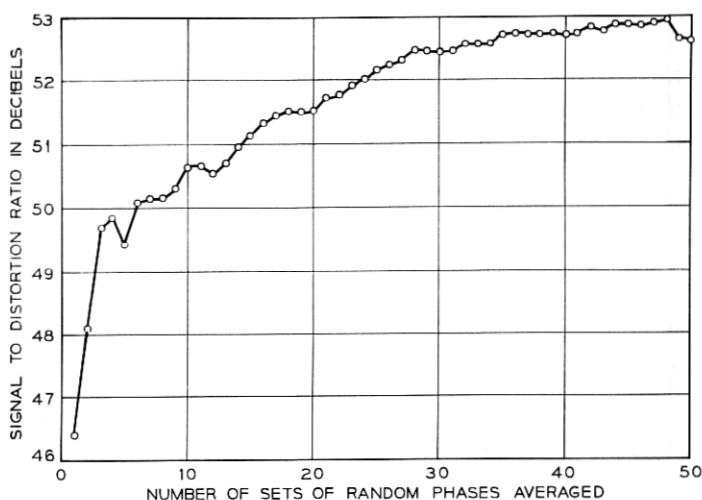


Fig. 12—Fluctuations in SDR of single pole filter as a function of number of sets of computations. 50 sine waves in baseband; SDR computed in slots 17 + 19; bandwidth expansion factor $k = 10$; $\sigma = 0.2$ MHz; $\omega_c/W = 1.223$.

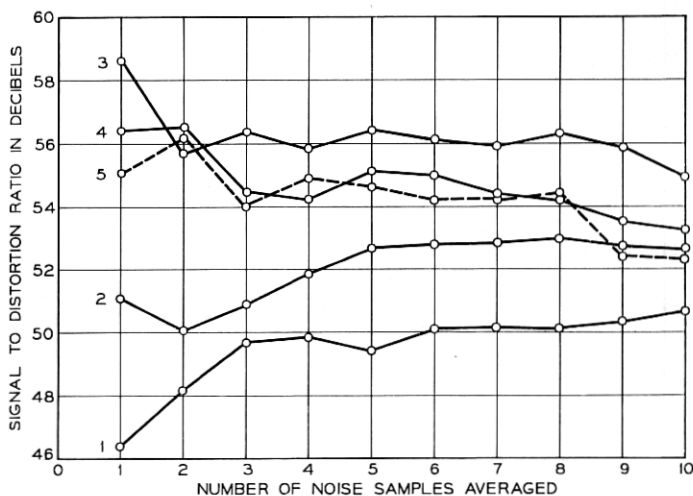


Fig. 13—Fluctuations in SDR of single pole filter as a function of number of sets of computations. 50 sine waves in baseband; SDR computed in slots 17 + 19; bandwidth expansion factor $k = 10$; $\sigma = 0.2$ MHz; $\omega_c/W = 1.223$.

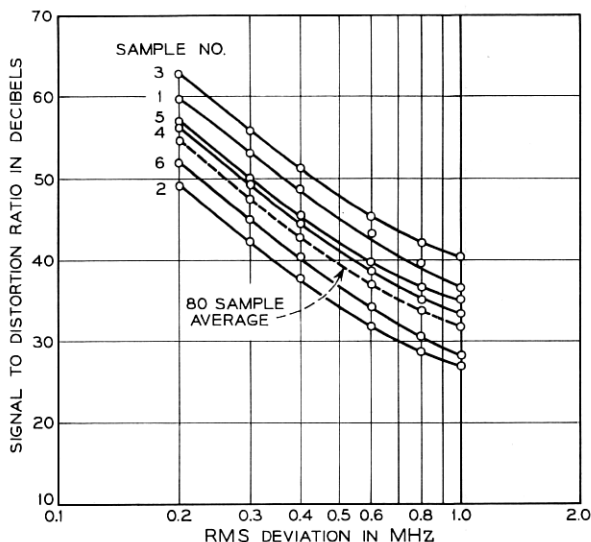


Fig. 14—Behavior of the SDR in a single noise sample as a function of σ/W . Single pole filter; slot 4; $N = 10$; sample set 1.

average. The same behavior has been observed for other filters. It is clear that almost any noise sample will predict the SDR behavior as a function of σ/W , but the actual SDR computed for the single noise sample depends on the peakiness of the sample.

V. THE THREE-POLE MAXIMALLY FLAT AMPLITUDE FILTER

The maximally flat amplitude filter is used widely in frequency modulation systems; it has the flattest possible amplitude response near the midband frequency and is often used in conjunction with a phase equalizer. The transfer function of a narrow band three-pole bandpass filter is

$$Y = \frac{1}{1 - b_2 \left(\frac{f - f_o}{f_c} \right)^2 + j \left(\frac{f - f_o}{f_c} \right) \left[b_1 - \left(\frac{f - f_o}{f_c} \right)^2 \right]} \quad (15)$$

where

f_o is the midband frequency and

f_c is the filter half bandwidth; that is, the frequencies at which the response is down 3 dB are $f_o \pm f_c$,

b_1, b_2 are both equal to 2 for an MFA filter.

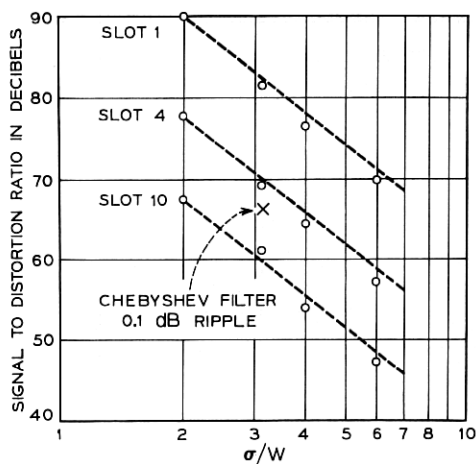


Fig. 15—FM signal-to-distortion ratios in a three-pole MFA filter. $W = 7$ MHz; 3 dB filter bandwidth = 238 MHz; $N = 10$; $k = 50$; no carrier offset.

SDR computations for an unequalized filter are presented in Fig. 15 as a function of frequency deviation. The dashed lines are 12 dB per octave slopes placed arbitrarily to coincide with the data at $\sigma/W = 2$. The data points are 20-sample averages. The large cross is the SDR in slot 10 of a three pole 0.1 dB ripple Chebyshev filter with the same skirt selectivity as the MFA filter at a frequency 256

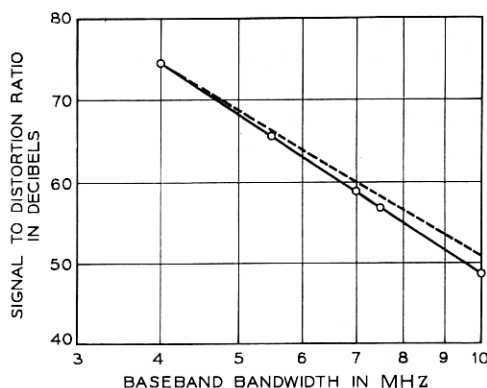


Fig. 16—FM signal-to-distortion ratios in a three-pole MFA filter. $\sigma/W = 3.12$; 3 dB filter bandwidth = 238 MHz; $N = 10$; $k = 30$; slot 10; no carrier offset.

MHz from the carrier. The Chebyshev filter is clearly superior to the MFA filter in this instance. The SDR is a function of baseband W as shown in Fig. 16 for $\sigma/W = 3.12$ and slot 10. An arbitrary slope of 18 dB per octave is included. As in Fig. 15, the data points are 20-sample averages.

Fig. 17 shows the effect of a carrier frequency offset with respect to the filter midband frequency. In the application for which this filter was chosen, the midband frequency change over the ambient temperature range -40°F to $+140^{\circ}\text{F}$ is about ± 6 MHz.

Results for perfect phase equalization are shown in Fig. 18; arbitrary slopes have been added. It is clear that nearly all of the distortion in the unequalized filter is due to nonlinear phase.

VI. AMPLITUDE TO PHASE CONVERSION

In addition to the FM distortion in the filter output there is generally some envelope distortion. Since all known limiters convert envelope modulation to phase modulation this source of distortion must be accounted for in system design. The envelope distortion is computed as described in Section II and it is necessary to relate it to the AM/PM conversion of the limiter.

For good limiters the AM/PM conversion is small and can be assumed linear, that is,

$$\theta = Qm \quad (16)$$

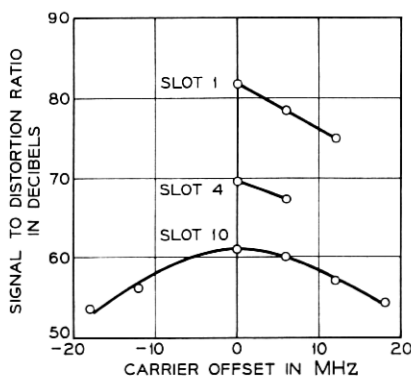


Fig. 17 — FM SDR in three-pole MFA filter as a function of carrier offset. $W = 7$ MHz; 3 dB filter bandwidth = 238 MHz; $N = 10$; $k = 50$; $\sigma/W = 3.12$.

where

m is the index of amplitude modulation for the slot of interest,
 θ is the phase shift in radians in the same slot caused by m , and
 Q is the AM/PM conversion coefficient.

The normal signal in the slot of interest is a sine wave of amplitude A . The signal-to-AM/PM distortion ratio is given by

$$\begin{aligned}\text{SDR (AM)} &= 20 \log A/\theta \\ &= 20 \log A/Qm \\ &= 20 \log A/m - 20 \log Q.\end{aligned}\quad (17)$$

The first term, $20 \log A/m$, can be computed for the network and the AM/PM conversion coefficient can be included separately.

The AM and FM SDR's for transitional Butterworth-Thomson filters¹² are plotted in Fig. 19. For the Chebyshev filter the AM and FM SDR are 72.3 and 66.3 dB, respectively. All filters were adjusted for equal loss 256 MHz from the midband frequency. The trends are

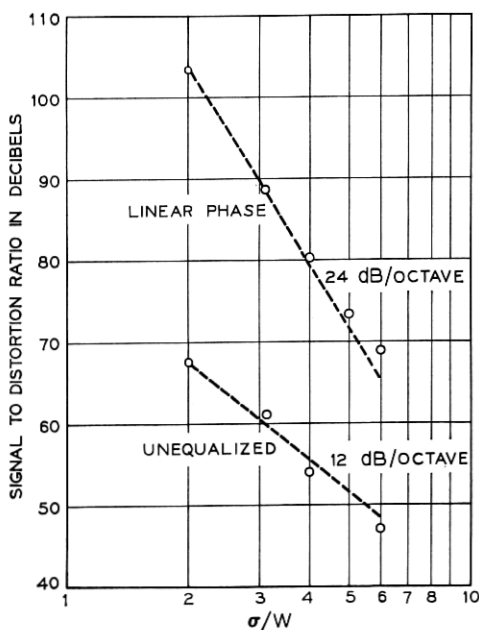


Fig. 18—FM SDR in a phase-equalized three-pole MFA filter. $W = 7$ MHz; 3 dB bandwidth = 238 MHz; $N = 10$; $k = 50$; slot 10.

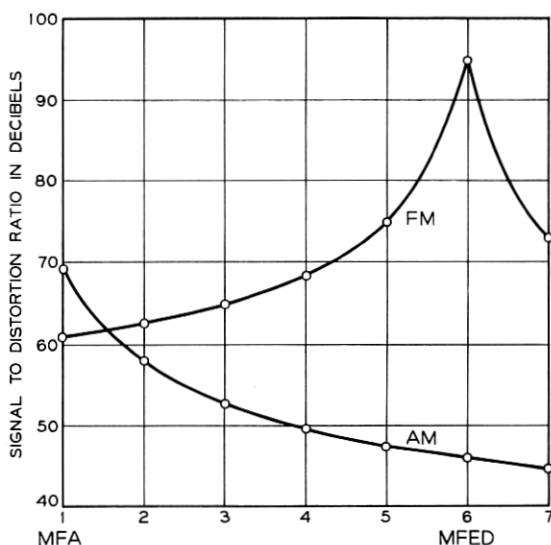


Fig. 19 — FM and AM SDR in three-pole transitional Butterworth-Thomson filters. $W = 7$ MHz; loss 256 MHz from midband = 20 db; $N = 10$; $k = 30$; no carrier offset; $\sigma/W = 3.12$; slot 10.

as expected, as the filter goes from MFA to maximally flat envelope delay (MFED) the FM distortion decreases and the AM/PM distortion increases. The effect of the limiter AM/PM conversion coefficient can be included by adding $-20 \log Q$ to the curve marked AM.

The frequency responses for the filters are given by (15); for the 0.1 dB ripple Chebyshev filter $b_1 = 1.921$, $b_2 = 1.801$. For the transitional Butterworth-Thomson filters the parameters are:

Filter No.	1-MFA	2	3	4	5	6-MFED	7
b_1	2.0	2.103	2.201	2.294	2.383	2.466	2.547
b_2	2.0	2.092	2.182	2.268	2.352	2.433	2.510

VII. DISCUSSION

The Fourier method for the computation of FM distortion in linear networks has been described and some results presented for single sine wave modulation and for random noise modulation simulated by groups of harmonically related sine waves. The method is exact to an accuracy determined by the round-off error in the machine.

Although the computation is exact for any individual input signal, the results for noise modulation are only approximate because the results depend upon averaging over a finite number of periodic noise samples. Much of the work described in this paper has been devoted to describing the behavior of the noise computations and in the determination of the maximum modulation index for which computations can be made with suitable accuracy.

In addition to demonstrating the nature of convergence of the noise averaging method, a detailed comparison of this method with the experimental results of W. F. Bodtmann provides an excellent demonstration of the extent to which a noise sample consisting of as few as 10 sine waves approximates a thermal noise signal. The noise simulation with a 10 sine wave noise sample is sufficient for most applications and accurate computations have been made for modulation indexes of $\sigma \leq 6W$ where σ is the rms frequency deviation and W is the bandwidth of the modulating signal.

It is notable that a single periodic noise sample is sufficient to determine the shape of the curve describing the signal-to-distortion ratio as a function of the deviation, the baseband bandwidth, or the filter parameters. This result, illustrated in Fig. 14, can be used to conserve computational time when optimizing the parameters of a system.

ACKNOWLEDGMENTS

I am indebted to M. V. Schneider who guided me patiently through the programming maze as far as I have gone, and to T. L. Osborne who insisted from the beginning that the Chebyshev 0.1 dB ripple filter was better than my choice of the MFA filter.

REFERENCES

1. Roder, H., "Effects of Tuned Circuits Upon a Frequency Modulated Signal," *Proc. I.R.E.*, 25, No. 12 (December 1937), pp. 1617-1647.
2. Stumpers, F. W. L. M., "Distortion of Frequency Modulated Signals in Electrical Networks," *Commun. News*, 9, No. 3 (April 1948), pp. 82-92.
3. Panter, P. F., *Modulation, Noise, and Spectral Analysis*, New York: McGraw-Hill, 1965, pp. 273-280.
4. Medhurst, R. G., and Roberts, J. H., "Evaluation of Distortion in FM Trunk Radio Systems by a Monte Carlo Method," *Proc. I.E.E.*, 113, No. 4 (April 1966), pp. 570-580.
5. Rice, S. O., "Mathematical Analysis of Random Noise," *B.S.T.J.*, 23, No. 3 (July 1944), pp. 282-332, and 24, No. 1 (January 1945), pp. 46-156.
6. Bennett, W. R., "Distribution of the Sum of Randomly Phased Components," *Quart. Appl. Math.*, 5, No. 1 (April 1947), pp. 385-393.
7. Enloe, L. H., "Decreasing the Threshold in FM By Frequency Feedback," *Proc. I.R.E.*, 50 (January 1962), pp. 18-30.

8. Bodtmann, W. F., unpublished work.
9. Enloe, L. H., and Ruthroff, C. L., "A Common Error in FM Distortion Theory," Proc. I.E.E.E., 51, No. 5 (May 1963), p. 846.
10. Gladwin, A. S., Medhurst, R. G., Enloe, L. H., Ruthroff, C. L., "A Common Error in FM Distortion Theory," Proc. IEEE, 52, No. 2 (February 1964), pp. 186-189.
11. Magnusson, R. I., Enloe, L. H., Ruthroff, C. L., "A Common Error in FM Distortion Theory," Proc. IEEE, 52, No. 9 (September 1964) pp. 1082-1084.
12. Peless, Y., Murakami, T., "Analysis and Synthesis of Transitional Butterworth-Thomson Filters and Bandpass Amplifiers," RCA Review, 18, No. 1 (March 1957), pp. 60-94.

